Khati et al. Journal of Analytical Science and Technology (2018) 9:24
https://doi.org/10.1186/s40543-018-0156-y

Journal of Analytical Science and Technology

RESEARCH ARTICLE Open Access

Electro-capacitive performance of haemoglobin/polypyrrole composites for high power density electrode

Komal Khati*, Ila Joshi and Mohammad Ghulam Haider Zaidi

Abstract

Background: Haemoglobin (Hb)-doped polypyrrole (PPy) composites serving as energy storage material have rarely been premeditated.

Methods: In this perspective, a novel class of haemoglobin/polypyrrole composites (HPyCs) by doping metal derivative Hb into PPy matrix with concentrations (PPy, 1%, 2% and 3% Hb in *w/w*) has been synthesized by cationic surfactant assisted dilute polymerization method. The obtained samples were exemplified by Fourier transform-infrared spectroscopy (FT-IR) and thermogravimetric-differential thermal analysis-differential thermogravimetry (TG-DTA-DTG). Electrochemical capacitance (Cs, F/g) of electrodes fabricated from PPy and HPyCs over stainless steel in the presence of sulphonated polysulphone as binder has been investigated in KOH solution (1.0 M) with reference to Ag/AgCl at scan rate (V/s) ranging 0.001–0.2. HPyC3% has shown Cs of 445.75F/g along with energy and power densities of 14.37 Wh/kg and 596.54 Wh/kg respectively, which is greater as compared to 200.56F/g for PPy.

Conclusion: The composites show good charge-discharge with improved electrochemical cyclic stability of the HPyCs over PPy. This behaviour points out that fabricated HPyCs may dole out as prospective electrode materials for development of electrochemical supercapacitors.

Keywords: Polypyrrole, Haemoglobin, Electrochemical capacitance, Sulphonated polysulphone

Background

The scarceness of power owing to emergent masses, undue worldwide upgrading and energy expenditure in domestic and industrialized areas may elevate the demand for energy storage devices (Ramachandran et al. 2015; Wang et al. 2012).Therefore, the improved energy-sustainable and energy-efficient economy depends on the ability to produce novel materials for electrochemical supercapacitor (Ghosh et al. 2016). In modern period, the polymer composites (PCs) have engrossed considerable interest globally due to their scientific and technical use in electrochemical power supply such as automotives, fuel cells, handy electronics, batteries and supercapacitors (Hanemann and Szabó 2010). For preeminent viable preservation and storage of electrochemical energy, there has been rising requirement of PCs derived through doping of metal ions into conducting polymer-bearing enhanced electrical conductivity (Mane et al. 2014), dielectric (Guo et al. 2013), thermoelectric properties (Du et al. 2012), sensory (Maity and Chatterjee 2015) and supercapacitors application (Ghosh et al. 2016).The condensed over-potential along with high rates of charge-discharge and extended cyclic stability are the primary aspects of such prepared PCs (Ramachandran et al. 2015).

Intrinsically conducting polymers with conjugated double bonds have attracted much consideration as advanced materials (Wang et al. 2001). Among these, PPy has been regarded as predictive material expansively studied with respect to its commercial appliances due to its high surface area, low cost, ease of polymerization and good stability that can be regulated by doping (Deng et al. 2014; Qian et al. 2013; Snook et al. 2011). In earlier studies, PPy doped 2,2′-bipyridine (Thakur and Lokhande 2018a), $Cu(OH)_2$ (Thakur and

* Correspondence: komal.chem89@gmail.com
Department of Chemistry, G. B. Pant University of Agriculture and Technology, Pantnagar, Uttarakhand 263 145, India

Lokhande 2017a), MnO_2 (Li et al. 2010), CeO_2 (Wang et al. 2016), TiO_2 (Gao et al. 2014), RuO_2 (Zang et al. 2008), Fe (Cysewska et al. 2015), Fe_2O_3 (Navale et al. 2014), Porphyrin (Zhou et al. 2007) and Hb (Baghayeri et al. 2015). Recently, work reported on V_2O_5 (Ingole and Lokhande 2016), FeO(OH) (Thakur and Lokhande 2018b and Fe_3O_4 (Thakur and Lokhande 2017b) as electrode materials deposited on stainless steel for the improvement of supercapacitance and battery applications. In this perspective, macrocyclic metal ion Hb functionalized PPy has been investigated as electrode materials in the development of high power energy storage systems.

Hb electron transfer reaction is an attractive topic because of its wide applications in biosensors, bioelectronics and energy storage systems. It is an imperative redox respiratory protein in red cells and composed of four polypeptide chains, each has one iron heme group (Scheller et al. 2005). Due to its commercial ease of utilization, known structure, judicious cost, high stability and capability rate, Hb is considered as an ideal model for the study of electrochemical performance for supercapacitor (Khairy and El-Safty 2014).

The present study has put emphasis on the simplified approach towards preparation of novel HPyCs through CTAB-assisted polymerization of Py in the presence of different concentrations of Hb (%, *w*/*w*) ranging 1–3 at 30 ± 1 °C in aqueous medium. The process of polymerization was initiated with $FeCl_3$ that serves as oxidant (Mudila et al. 2013). Fabrication of HPyCs, its characterization through spectral FT-IR and TGA-DTA-DTG suggest the interaction of Hb moiety in PPy matrix and thermally stable behaviour of composites. The synthesized HPyCs have shown their significance as a high power electrode material with ~ 1.5% electro-capacitive decrease during the first 1000 cycles at scan rate of 0.1 V/s. To the best of our information, we exhibit foremost, the electrochemical supercapacitance behaviour of the proposed HPyCs. New and interesting results were observed with increasing concentration of Hb in the matrix of PPy, suggesting its importance as a potential entrant for upcoming generation for energy strategies.

Methods

Chemicals and reagents

Commercially available haemoglobin (Otto Kemi, India), pyrrole (> 99% Across Chemicals), polysulphone (Mw; 16×10^3), CTAB (> 99% sd. Fine Chemical India), graphite (> 98.0%, 500 μm Loba Cheme India), and chlorosulphonic acid (> 99% Sigma Aldrich). Other chemicals and solvents were obtained from S.D. Fine Chemicals India.

Preparation of SPS

SPS applied as binder and one of the constituent in the matrix was synthesized through sulphonation of polysulphone resin (PSO) with chlorosulphonic acid in dichloromethane as illustrated (Unnikrishnan et al. 2012). The precipitated SPS was filtered off and repeatedly washed with aqueous solution of sodium hydroxide (10%, *w*/*v*) for the exclusion of unreacted chlorosulphonic acid. Ultimately, the polymer was washed with distilled water to eradicate traces of solvent until neutral water was obtained and dried at 80 ± 1 °C overnight.

Synthesis of HPyCs

All the HPyCs were synthesized by CTAB-assisted dilute polymerization in a thermostatically controlled glass reactor equipped with mechanical stirrer, thermometer and a dropping funnel. The suspension of Py in de-ionized water (0.12 mol/dL) stabilized with CTAB (1.15 g, 3.50×10^{-3} mol) was placed in the reactor. To this, the necessitate concentration of Hb (1–3%, *w*/*w*) was added and contents were stirred @ 500 rpm over 15 min at 30 ± 1 °C. Meanwhile, the aqueous solution of $FeCl_3$ (30 mL, 1.85×10^{-2} mol/dL) in deionized water was added drop wise to the suspension of Py. The polymerization process was allowed to progress @ 500 rpm over 24 h at 30 ± 1 °C. The formation of HPyCs was determined through appearance of black colour precipitate. HPyCs with ≥ 95% yield were separated through filtration from the reaction mixture and washed with distilled water until pale filtrate was achieved. The obtained HPyCs were dried at 60 ± 1 °C/400 mmHg over 8 h. Following the aforementioned method, HPyCs were synthesized with doping (%, *w*/*w*) 1–3 of Hb respectively. PPy was also synthesized in 85% yield under identical conditions (Mudila et al. 2013).

Fabrication of working electrodes

Prior to deposition, commercially available 316-SS with 1 cm^2 area (mesh size 320,600) and 0.16 mm thickness was well polished with emery paper followed by cleaning the surface with acetone. Stainless steel(SS) were fabricated through coating a composition of electroactive material (70 mg) along with graphite (10 mg) which was added to a solution of an effective binder SPS (5 g/dL) in *N*-methyl Pyrollidone. The contents were ultrasonicated for 15 min. The mass loading slurry (100 μl) was condensed on a SS substrate which acts as a current collector. The treated substrate was desiccated at room temperature for 4 h followed by drying at 60 °C/400 mmHg for 48 h. This has afforded working electrodes with mass thickness of electroactive materials by 0.05 ± 0.01 mg over SS substrate. The electrodes were analyzed after 24 h of fabrication (Mudila et al. 2013).

Characterizations

Fourier transform-infrared (FT-IR) spectra were recorded over Thermo Nicolet in KBr. Simultaneous thermogravimetric-differential thermal analysis-differ ential thermogravimetry (TG-DTA-DTG) data were documented over EXSTAR TG/DTA 6300 at sample size (mg) ranging 8–11.2 @ 10 °C/min in air.

The electrochemical measurements were recorded over IVIUM Potentiostat-Galvanostat Netherlands BV at current compliance 1mA, voltage ranging -0.1 to -0.6V at scan rate (V/s) of 0.001-0.2. The electrochemical properties, capacitive behaviour and stability of electrodes were studied by Cyclic Voltammetry (CV) and Electron Impedance Spectroscopy (EIS). All the electrochemical performance were analysed in a three electrode cell assembly equipped with reference to Ag/AgCl, Pt foil (1cm2 area) as counter electrodes and working electrode in KOH solution (1.0M). Cs of materials was calculated from the voltammetric charges by the CV curve, according to relation:

$$\mathrm{Cs} = \mathrm{qa} + |\mathrm{qc}| / 2m\Delta \mathrm{V} \quad (1)$$

where qa and qc are the voltammetric charges on anodic and cathodic scans in the capacitive potential region (ΔV) and m being the mass of electroactive material.

Results and discussion

FT-IR spectra

Figure 1 reveals FT-IR spectra of PPy, Hb and respective HPyC3%. It may be deduced that most of the assignments of PPy are maintained in the HPyC3% spectra from 500 to 1750 cm^{-1}. Hb shows characteristic absorptions at νO–H (3289 cm^{-1}) which departed in the spectra of HPyC3%, thus verifying the interaction of secondary amino group of PPy with carboxylic group of Hb moiety. The other characteristic absorption of Hb are νC=O (1652.00 cm^{-1}), νC–N (1541 cm^{-1}), νC–O (612 cm^{-1}) (Aboul-Enein et al. 2014; Kong and Yu 2007), and νC–H (2927 cm^{-1}). PPy shows characteristic FT-IR absorptions resultant to νN–H (3450.10 cm^{-1}) (Jiwei et al. 2008), νC–H (2925.10 cm^{-1}) (Sonavane et al. 2010), symmetrical νC=C (1652.10 cm^{-1}), νC–C (1463.20 cm^{-1}) and νC–N (1513.20 cm^{-1}) (Sonavane et al. 2010). These absorption peaks correspond to the formation of 2, 5-substituted PPy (Qiao et al. 2010; Ramachandran et al. 2015), νC–H (1397 cm^{-1}) in-plane bending (Qu et al. 2010) and νC–H out of plane bend (932 cm^{-1}) (Ramachandran et al. 2015). Doping induced bands associated with conjugated backbone for PPy appeared at 1160.40 cm$^-$1 (Liu et al. 2005; Yang et al. 2011). HPyC3% shows characteristic absorption peak at νN–H (3402 cm^{-1}), νC–H (2917 cm^{-1}), νC=O (1655 cm^{-1}) and νC–N (1528 cm^{-1}) are nearly similar to that of Hb. For further qualitative phase interaction of Hb into PPy matrix was investigated through Scanning Electron Microscope (SEM) micrograph mentioned in Additional file 1.

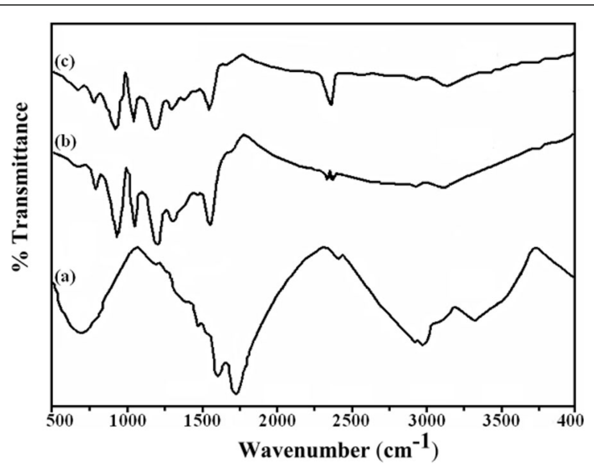

Fig. 1 FT-IR spectra of (**a**) Hb, (**b**) PPy and (**c**) HPyC3%

Thermal characteristics

The TGA curve of PPy, Hb and PPy/Hb with 3% Hb is shown in Fig. 2a. In the case of PPy, the weight loss was observed in two stages at 200 °C (13.04%) and at 300 °C (100%); the first one was due to physisorbed water molecule and volatile impurities while the second one was due to the degradation of unsaturated group in polymer (Jakab et al. 2007; Basavaraja et al. 2009). In the case of Hb, first weight loss was observed at 190 °C (9.1%), second weight loss was observed at 339 °C (42.6%) and third weight loss was found at 504 °C (50.7%). In PPy/Hb composite, the first weight loss at 200 °C (11.73%) is due to removal of oligomer molecules and second weight loss up to 590 °C (27.75%) is because of degradation of PPy. The minimum loss of Hb from PPy/Hb is responsible for higher thermal stability of the composite material. Figure 2b shows the DTA curve of pure PPy, Hb and PPy/Hb. Due to polymeric degradation of material, a broad exothermic peak ranging from 264 to 582 °C and 268 to 597 °C was observed in PPy and PPy/Hb respectively. Shifting of the exothermic peak in PPy/Hb assures the results of TGA indicating higher thermal stability of PPy/Hb. The comparative DTG analysis of PPy, Hb and PPy/Hb composite as derivatized weight loss vs. temperature is shown in Fig. 2c.

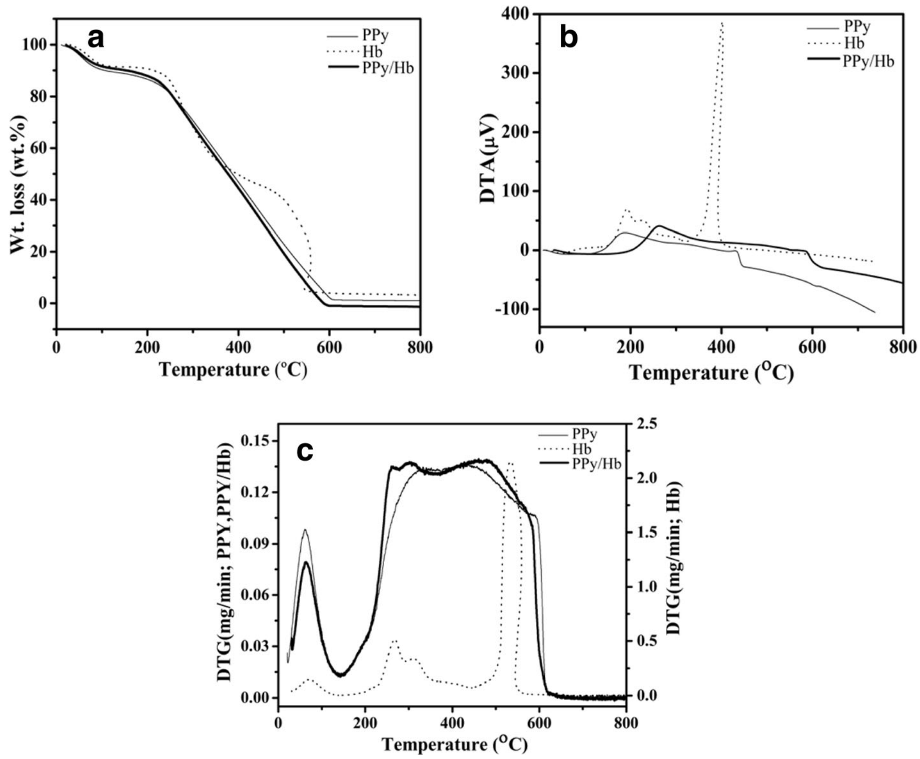

Fig. 2 **a** TGA. **b** DTA. **c** DTG

Weight loss of PPy decomposition was observed at 65 °C and 260 °C to 575 °C with 79 μg/min and 135 to 107 μg/min weight losses respectively whereas in case of Hb decomposition weight loss was found with 0.51 to 0.33 mg/min at 267 to 316 °C and 2.13 mg/min at 530 °C respectively. However, in the case of PPy/Hb, the decomposition was found 92 μg/min at 62 °C and 128 to 106 μg/min from 301 to 590 °C respectively. Thus, it could be inferred from DTG studies that rate of thermal decomposition was lower in the case of PPy/Hb, whereas higher in the case of PPy. The higher thermal resistance of PPy/Hb was due to incorporation of Hb in the PPy matrix.

Electrochemical analysis

Electrochemical studies on Hb, PPy and respective HPyCs electrodes with (%,*w*/*w*) ranging 1–3 deliver us exciting conclusions which demonstrate HPyCs as quite proficient material for preparation and its development as a material for energy storage devices. All the materials signify voltammogram in the voltage range of − 0.6 to − 0.1 V at different scan rates (V/s) of 0.001–0.2 in

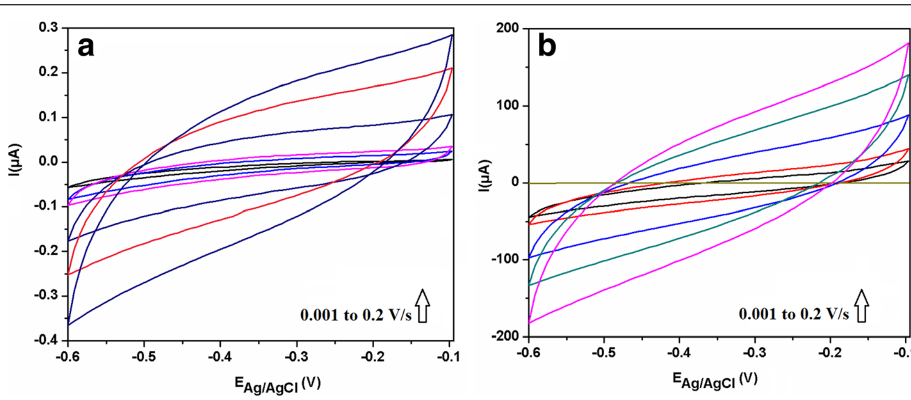

Fig. 3 CV of **a** Hb and **b** PPy at various scan rates

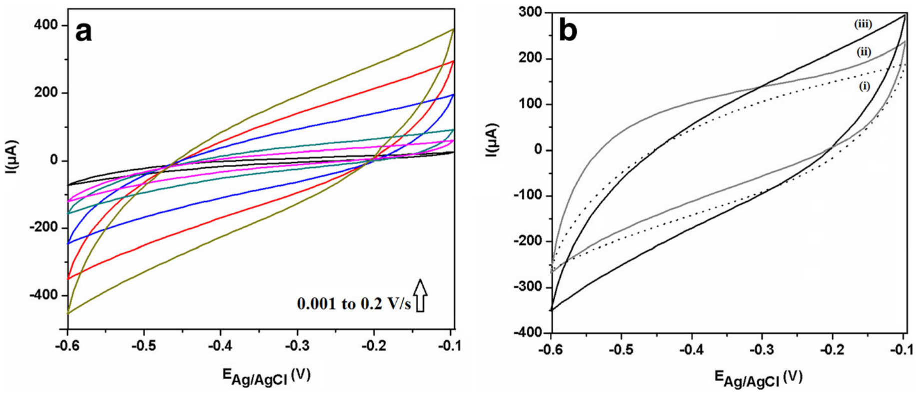

Fig. 4 CV of **a** HPyC3% at all scan rates. **b** CV of HPyCs 1–3% (i–iii) at 0.01 V/s

1.0 M KOH close to a rectangular shape with no current peak, which indicates a distinctive capacitive behaviour with fine charge propagation (Ghosh et al. 2016; Ramya et al. 2013). Hb has been predictable to involve flourishing ability and a prospective material to accumulate energy (Khairy and El-Safty 2014). The CV was taken in the above held potential range to provide specific capacitance of 3.20 to 0.20 F/g (Fig. 3b). With scan rates, a regular increase in the peak currents has been observed for PPy electrodes and the Cs ranges from 200.56 to 14.80 F/g in Fig. 3a. Figure 4a exhibits the intensification in specific capacitance for HPyC3% which has been ranged from 445.75 to 20.60 F/g. With increasing portion of Hb (1–3% *w*/*w*) in the matrix of polymer, a steady increase was observed in the specific capacitance of HPyCs at 0.01 V/s (Fig. 4b). Figure 5a illustrates the comparative specific capacitance of Hb, PPy and HPyC3% at scan rate of 0.01 V/s which demonstrate HPyC3% to be most supercapacitive which is further confirmed with the comparative histogram of Cs of all the materials (Fig. 5b). The increase in the capacitance of HPyCs may be attributed to the formation of synergistic effect among secondary amine group of PPy with carboxylic group of Hb moiety, which augment the surface active sites of the HPyCs. Such HPyCs consequently amplify the active material usage as of speedy electron transfer in addition to the storage accumulation for ions. On the contrary, the decrease of capacitance with increasing scan rate in CV curves can be elucidate to the fact that, at elevated scan rate, charge dispersion is not able to pursue the variant in electric field and thus proceeds small capacitance or energy density and high power density.

The energy density (E) and power density (P) for PPy and HPyC3% were estimated respectively through following equations:

$$E = \frac{Cs(\Delta V)^2}{2} \tag{2}$$

$$P = \frac{E}{\Delta t} x3600 \tag{3}$$

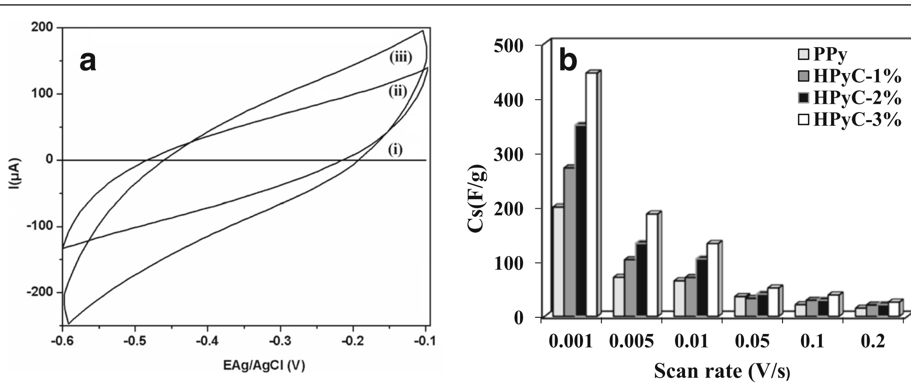

Fig. 5 a CV of Hb, PPy and HPyC3% (i–iii) at 0.01 V/s. **b** Specific capacitance of all materials

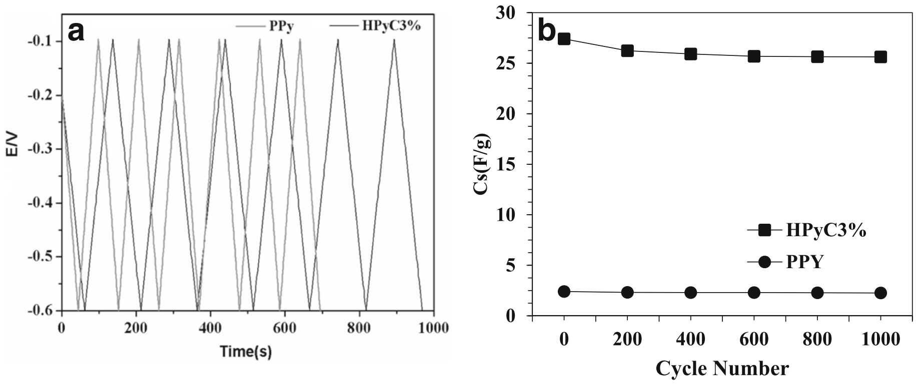

Fig. 6 a Charge-discharge curves. **b** Effect of number of cycle on the Cs and stability

where "Cs" is specific capacitance, ΔV is the applied initial voltage and "Δt" is the corresponding discharge time in hour (Fu et al. 2018; Mudila et al. 2017). The maximum energy density of 6.26 Wh/kg and 14.37 Wh/kg was encountered for PPy and HPyC3%, while the corresponding power density of 259.76 W/kg and 596.54 W/kg was reported respectively.

Figure 6a shows charging-discharging curves of PPy and HPyC3% recorded in the voltage range from − 0.6 to − 0.1 V at an applied current density of 10 mA/cm^2. The charge/discharge curves exhibit reversible characteristics devoid of noticeable deviation in each cycle; these charge/discharge curves are almost linear in the total range of potential with constant slopes, signifying perfect electro-capacitive behaviour. This suggests good electrochemical stability for the HPyCs electrodes with a capacitive decrease of 1.5% during the first 1000 cycles at a scan rate of 0.1 V/s that indicates improved cyclic stability of the HPyCs over PPy (Fig. 6b), making them appropriate for improvement of electrochemical supercapacitors (Table 1). Electrochemical Impedance Spectroscopy (EIS) was performed to determine the parameters for electron transfer reactions at the interface of the working electrode. EIS spectra of PPy and HPyC3% are measured in the frequency ranges from 0.1 to1000 Hz with pulse amplitude of 0.03 mV. Nyquist diagram for the PPy and HPyC3% electrodes are shown in Fig. 7. The Nyquist diagram of both the electrodes consist of the two parts, one is quasi semicircle in the high frequency region and another shows linear part at low frequency region. The electrolyte resistance (Rs), can be found from the semicircle interception point on the real axis while the charge transfer resistance (Rct), was calculated by measuring the magnitude of the diameter of semicircle on the electrode surface. PPy illustrate high impedance values compared with those obtained for the HPyC3%. The curves achieved for the HPyC3% also showed a deviation in slope from a vertical position in relation to PPy, which is attributed to the low *R*ct values and may be ascribed to the high porosity and mobility inside the electrodes. This supports electronic transfer in the HPyCs, thus significantly reducing the *R*ct value, making it more capacitive. The increase in electron transfer in HPyC3% is perhaps attributable to the charge transfer between Hb and PPy. This can be partly proven by the FT-IR spectrum, which suggests interaction of electrons

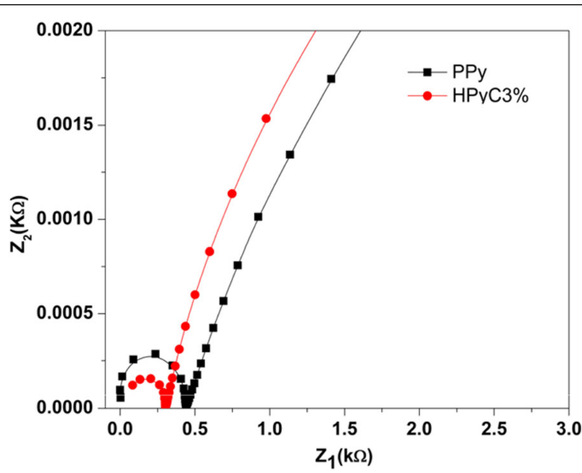

Fig. 7 Nyquist plots of PPy and HPyC3%

Table 1 Performance comparison of Hb-based PPy supercapacitors. The table shows the comparison of electrochemical performance of reported PPy and HPyCs in this work

S.No.	Name of materials	Electrolyte	Cs(F/g)	Current density (mA/cm^2)	Energy density (Wh/Kg)	Power density (W/Kg)
1	PPy	1.0 M KOH	200.56	10	6.26	259.76
2	HPyC3%	1.0 M KOH	445.75	10	14.37	596.54

among Hb and PPy. Also, due to the large surface area of Hb, may serve as linking PPy and results in higher conductivity, thus lowering the *R*ct values obtained for HPyC3%. The Rs and Rct for HPyC3% is less than the PPy, which conclude that HPyCs is highly conductive as well as fairly stable as an electrode material.

Conclusions

A series of haemoglobin/polypyrrole composites (HPyCs) were prepared through $FeCl_3$-assisted dilute polymerization of Py. The FT-IR reveals the physical interface between the two and TG-DTA-DTG informs the thermal assets of HPyCs which get more stable with percentage of Hb. CV studies suggest that these HPyCs having varying concentration of Hb (1–3%) in their matrix can be employed as potential material for the above said property. HPyC3% had provided with specific capacitance of 445.75F/g which is higher compared to PPy that comprises of capacitance of 200.56F/g. The consecutive scans of HPyC3% electrode for 1000 cycles at the scan rate of 0.1 V/s in KOH (1.0 M) with capacitive retention of ~ 98.5% illuminating good cyclic stability of electrode material. The charge-discharge curves are nearly linear in the total range of potential with constant slopes, presenting idyllic electro-capacitive behaviour. The maximum energy density of 6.26 Wh/kg and 14.37 Wh/kg was encountered for PPy and HPyC3%, while corresponding power density of 259.76 W/kg and 596.54 W/kg was reported respectively. The HPyCs showed the lowest impedance values and charge-transfer resistance compared to the PPy, indicating that electron transfer in the HPyCs was favoured by an association between the constituent materials. The present effort demonstrates a simple and cost-effective approach for synthesis of the electrochemically commercial HPyCs with improved capacitance. This gives an idea about the preparation of the electrode materials for the development of electrochemical energy storage devices.

Additional file

Additional file 1: SEM micrograph of PPy and HPyCs (DOCX 628 kb)

Abbreviations

CTAB: Cetyltrimethylammonium bromide; Hb: Haemoglobin; PCs: Polymer Composites; PPy: Polypyrrole; PSO: Polysulphone; SPS: Sulphonated polysulphone; SS: Stainless steel

Acknowledgements

The author would like to thank CSIR, India, for awarding JRF and SRF.

Funding

Not applicable

Availability of data and materials

Not applicable

Authors' contributions

KK and MGHZ conceived the plan. KK and IJ performed the experiments, fabrication of electrode and other electrochemical studies. KK, IJ and MGHZ performed the data analysis. KK, IJ and MGHZ did the manuscript writing and execute the data interpretation. All authors had read and agreed for the final manuscript.

Competing interests

The authors declare that they have no competing interests.

Publisher's Note

Springer Nature remains neutral with regard to jurisdictional claims in published maps and institutional affiliations.

Received: 1 August 2018 Accepted: 10 October 2018
Published online: 27 October 2018

References

Aboul-Enein Y, Bunaciu AA, Fleschin S. Evaluation of the protein secondary structures using Fourier transform infrared spectroscopy. GUJS. 2014;27(1):637–44.

Baghayeri M, Zare EN, Lakouraj MM. Monitoring of hydrogen peroxide using a glassy carbon electrode modified with hemoglobin and a polypyrrole-based nanocomposite. Microchem Acta. 2015;182(3–4):771–9.

Basavaraja C, Kim NR, Jo E, Pierson R, Huh DS, Venkataraman A. Transport properties of polypyrrole films doped with sulphonic acids. Bull Kor Chem Soc. 2009;30(11):2701–6.

Cysewska K, Virtanen S, JasiÅ SP. Electrochemica activity and electrical properties of optimized polypyrrole coatings on iron. J Electrochem Soc. 2015;162(12):307–13.

Deng H, Lin L, Ji M, Zhang S, Yang M, Fu Q. Progress on the morphological control of conductive network in conductive polymer composites and the use as electroactive multifunctional materials. Prog Polym Sci. 2014;39(4):627–55.

Du Y, Shen SZ, Cai K, Casey PS. Research progress on polymer–inorganic thermoelectric nanocomposite materials. Prog Polym Sci. 2012;37(6):820–41.

Fu C, Ma Q, Liu H, Tang W. Effects of graphene oxide on the conductivity and capacitance of Polypyrrole. Int J Electrochem Sci. 2018;13:4267–75.

Gao Y, Wang Y, Xu X, Ding K, Yu D. Synthesis of polypyrrole–titanium dioxide brush-like nanocomposites with enhanced supercapacitive performance. RSC Adv. 2014;4(109):63719–24.

Ghosh S, Maiyalagan T, Basu RN. Nanostructured conducting polymers for energy applications: towards a sustainable platform. NLM. 2016;8(13):6921–47.

Guo J, Gu H, Wei H, Zhang Q, Haldolaarachchige N, Li Y, Young DP, Wei S, Guo Z. Magnetite–polypyrrole metacomposites: dielectric properties and magnetoresistance behavior. J Phys Chem C. 2013;117(19):10191–202.

Hanemann T, Szabó DV. Polymer–nanoparticle composites: from synthesis to modern applications. Mater. 2010;3(6):3468–517.

Ingole RS, Lokhande BJ. Effect of pyrolysis temperature on structural, morphological and electrochemical properties of vanadium oxide thin films. J Anal Appl Pyrolysis. 2016;120:434–40.

Jakab E, Mészáros E, Omastová M. Thermal decomposition of polypyrroles. J ThermAnal Cal. 2007;88(2):515–21.

Jiwei L, Jingxia Q, Miao Y, Chen J. Preparation and characterization of Pt-polypyrrole nanocomposite for electrochemical reduction of oxygen. J Mater Sci. 2008;43(18):6285.

Khairy M, El-Safty SA. Hemoproteins–nickel foam hybrids as effective supercapacitors. Chem Commun. 2014;50(11):1356–8.

Kong J, Yu S. Fourier transform infrared spectroscopic analysis of protein secondary structures. Acta Biochim Biophys Sinica. 2007;39(8):549–59.

Li J, Cui L, Zhang X. Preparation and electrochemistry of one-dimensional nanostructured MnO_2/PPy composite for electrochemical capacitor. Appl Surf Sci. 2010;256(13):4339–43.

Liu L, Zhao C, Zhao Y, Jia N, Zhou Q, Yan M, Jiang Z. Characteristics of polypyrrole (PPy) nano-tubules made by templated ac electropolymerization. Eur Polym J. 2005;41(9):2117–21.

Maity S, Chatterjee A. Textile/polypyrrole composites for sensory applications. J Compos. 2015:2356–7252.

Wang LX, Li XG, Yang YL. Preparation, properties and applications of polypyrroles. React Funct Polym. 2001;47(2):125–39.

Mane AT, Navale ST, Pawar RC, Lee CS, Patil VB. Microstructural, optical and electrical transport properties of WO_3 nanoparticles coated polypyrrole hybrid nanocomposites. Synth Met. 2014;199:187–95.

Mudila H, Rana S, Zaidi MGH. Supercritical CO_2 aided polyindole-graphene nanocomposites for high power density electrode. Adv Mater Let. 2017;8(3):269–75.
Mudila H, Zaidi MGH, Rana S, Joshi V, Alam S. Enhanced electrocapacitive performance of graphene oxide polypyrrole nanocomposites. IJCAS. 2013; 4(3):139–45.
Navale ST, Khuspe GD, Chougule MA, Patil VB. Synthesis and characterization of hybrid nanocomposites of polypyrrole filled with iron oxide nanoparticles. J Phy Chem Solids. 2014;75(2):236–43.
Qian T, Yu C, Wu S, Shen J. A facilely prepared polypyrrole-reduced graphene oxide composite with a crumpled surface for high performance supercapacitor electrodes. J Mater Chem A. 2013;1(22):6539–42.
Qiao Y-S, L-Z S, Dou T, Hu M. Polymerization and characterization of high conductivity and good adhension polypyrrole films for electromagnetic interference shielding. Chinese J Poly Sci. 2010;28(6):923–30.
Qu B, Xu YT, S-j L, Zheng Y-F, Dai L-Z. Fabrication of Pt nanoparticles decorated PP-MWNTs composites and their electrocatalytic activity for methanol oxidation. Synth Met. 2010;160(7–8):732–42.
Ramachandran R, Chen SM, Kumar GG. An overview of electrochemical energy storage devices of various electrodes and morphological studies of supercapacitors. Int J Electrochem Sci. 2015;10(12):10355–88.
Ramya R, Sivasubramanian R, Sangaranarayanan MV. Conducting polymers-based electrochemical supercapacitors–progress and prospects. Electrochim Acta. 2013;101:109–29.
Scheller FW, Bistolas N, Liu S, Jänchen M, Katterle M, Wollenberger U. Thirty years of haemoglobin electrochemistry. Adv Colloid Interface Sci. 2005; 116(1−3):111–20.
Snook GA, Kao P, Best AS. Conducting-polymer-based supercapacitor devices and electrodes. J Power Sources. 2011;196(1):1–12.
Sonavane AC, Inamdar AI, Dalavi DS, Deshmukh HP, Patil PS. Simple and rapid synthesis of NiO/PPy thin films with improved electrochromic performance. Electrochim Acta. 2010;55(7):2344–51.
Thakur AV, Lokhande BJ. $C_{10}H_8N_2$-PPy hybrid flexible electrodes: SILAR synthesis and electrochemical study. J Mater Sci- Mater El. 2018a;29(2):1630–5.
Thakur AV, Lokhande BJ. Dip time-dependent SILAR synthesis and electrochemical study of highly flexible PPy-$Cu(OH)_2$ hybrid electrodes for supercapacitors. J Solid State Electrochem. 2017a;21(9):2577–84.
Thakur AV, Lokhande BJ. Electrolytic anion affected charge storage mechanisms of Fe_3O_4 flexible thin film electrode in KCl and KOH: a comparative study by cyclic voltammetry and galvanostatic charge–discharge. J Mater Sci- Mater El. 2017b;28(16):11755–61.
Thakur A V, Lokhande B J (2018b) Source molarity affected surface morphological and electrochemical transitions in binder-free FeO(OH) flexible electrodes and fabrication of symmetric supercapacitive device. Chem Pap 72 (6):1407–1415.
Unnikrishnan L, Madamana P, Mohanty S, Nayak SK. Polysulfone/C30B nanocomposite membranes for fuel cell applications: effect of various sulfonating agents. Polym-Plast Technol. 2012;51(6):568–77.
Wang G, Zhang L, Zhang J. A review of electrode materials for electrochemical supercapacitors. Chem Soc Rev. 2012;41(2):797–828.
Wang X, Wang T, Liu D, Guo J, Liu P. Synthesis and electrochemical performance of CeO_2/PPy nanocomposites: interfacial effect. Ind Eng Chem Res. 2016; 55(4):866–74.
Yang S, Shen C, Liang Y, Tong H, He W, Shi X, Zhang X, H-j G. Graphene nanosheets-polypyrrole hybrid material as a highly active catalyst support for formic acid electro-oxidation. NLM. 2011;3(8):3277–84.
Zang J, Bao SJ, Li CM, Bian H, Cui X, Bao Q, Sun CQ, Guo J, Lian K. Well-aligned cone-shaped nanostructure of polypyrrole/RuO2 and its electrochemical supercapacitor. J Phys Chem C. 2008;112(38):14843–7.
Zhou Q, Li CM, Li J, Cui X, Gervasio D. Template-synthesized cobalt porphyrin/ polypyrrole nanocomposite and its electrocatalysis for oxygen reduction in neutral medium. J Phys Chem C. 2007;111(30):11216–22.